

# A Novel Electrochemical Anodization Cell for the Synthesis of Mesoporous Silicon

N. Gostkowska-Lekner<sup>1,2\*</sup>, D. Wallacher<sup>1</sup>, N. Grimm<sup>1</sup>, K. Habicht<sup>1,2</sup>, and T. Hofmann<sup>1</sup>

<sup>1</sup>Helmholtz-Zentrum Berlin für Materialien und Energie GmbH, Hahn-Meitner Platz 1, 14109 Berlin, Germany

<sup>2</sup>Institut für Physik und Astronomie, Universität Potsdam, Karl-Liebknecht-Straße 24-25, 14476 Potsdam, Germany

\*corresponding author: natalia.gostkowska@helmholtz-berlin.de

**Abstract:** A novel design of an electrochemical anodization cell dedicated to the synthesis of mesoporous, single-crystalline silicon is presented. First and foremost, the design principle follows user safety since electrochemical etching of silicon requires highly hazardous electrolytes based on hydrofluoric (HF) acid. The novel cell design allows for safe electrolyte handling prior, during and post etching. A peristaltic pump with HF-resistant fluoroelastomer tubing transfers electrolytes between dedicated reservoirs and the anodization cell. Due to the flexibility of the cell operation different processing conditions can be realized providing a large parameter range for the attainable sample thickness, its porosity and the mean pore size. Rapid etching on the order of several minutes to synthesize micrometer-thick porous silicon epilayers on bulk silicon is possible as well as long-time etching with continuous, controlled electrolyte flow for several days to prepare up to 1000  $\mu\text{m}$  thick self-supporting porous silicon membranes. A highly adaptable, LabVIEW-based control software allows for user defined etching profiles.

## Introduction

Crystalline silicon with nanometer-sized pores in the range between 1 nm and 200 nm is commonly referred to as micro- and mesoporous silicon [1]. Its discovery dates back to 1956 [2] though its full potential was only recognized roughly 20 years later [3]. Since then, it found widespread applications in fundamental as well as applied science [4-7]. Among its appealing properties are biocompatibility, tunable surface chemistry, huge pore-surface to pore-volume ratios, controllable morphology as an earth abundant, non-toxic and cheap source material [1, 8-10]. It is this diversity in properties that led scientists and engineers to propose porous silicon on a technological level for micro- and nano-fluidic applications [11], novel electrodes for ion batteries [6, 12,13], solar cell technology [14, 15], on-chip heat management [16] and thermoelectric elements [17-19], photonic and sensor applications [48-50] and to consider photoluminescence-based cancer markers [20, 21]. On a more fundamental level, porous silicon emerged in recent decades as versatile host material to study the effect of nano-confinement on the structural and dynamical properties of condensed matter [5, 22-24]. For a detailed and comprehensive review of porous silicon and its role in fundamental and applied science, we refer the interested reader to references [5, 7, 25].

E-beam lithography [26-28], polymer-template processing in combination with reactive ion etching [29, 30], metal assisted etching [31-33] and dry etching [34-36] are sophisticated, modern approaches to nanostructure silicon with exceptionally high control of pore and pitch sizes as well as pore arrangement. However, these methods are often limited to the synthesis of thin films, time consuming, expensive and do not allow for scalable synthesis of macroscopic amounts of micro- and mesoporous silicon. Consequently, today electrochemical wet-etching [1, 7, 25, 39] of silicon appears still as the most effective, yet not the safest synthesis route.

The etching of macroscopic amounts of mesoporous silicon heavily relies on hydrofluoric (HF) acid-based electrolytes. No feasible substitute for this highly hazardous substance exists to etch silicon effectively. Consequently, safety concerns are at the forefront of any synthesis attempt involving HF. In short, any possible contact of the experimentalist with the electrolyte even accidentally must be avoided under any circumstances. Proper personal protective equipment, a safe working environment, proper safety training of the experimentalist and a carefully designed electrochemical etching cell are as mandatory as the proper HF first aid-kit in the laboratory.

In this article, we present a novel electrochemical etching cell for the synthesis of mesoporous silicon in hydrofluoric acid-based electrolytes. The cell design's primary objective is to guarantee safe working conditions for the experimentalist. For this purpose, it employs multi-wall containments for the electrolyte in combination with a peristaltic pumping system to transfer safely the electrolyte between the etching cell and the storage containers. A broad flexibility with respect to electrochemical synthesis conditions was also an important design goal. In this sense, the presented cell can be utilized to synthesize self-supporting mesoporous membranes as thin as several tens of micrometers. Etching of mesoporous epi-layers thicker than 1000  $\mu\text{m}$  on silicon substrates becomes equally possible. A customized control software allows to run user-defined etch profiles. This article is organized as follows: We discuss first the design of the etching cell and elaborate on its benefits. Subsequently, we introduce the LabVIEW-based control software before we move on to a detailed description of cell handling. First synthesis results conclude our article.

## **Cell Design**

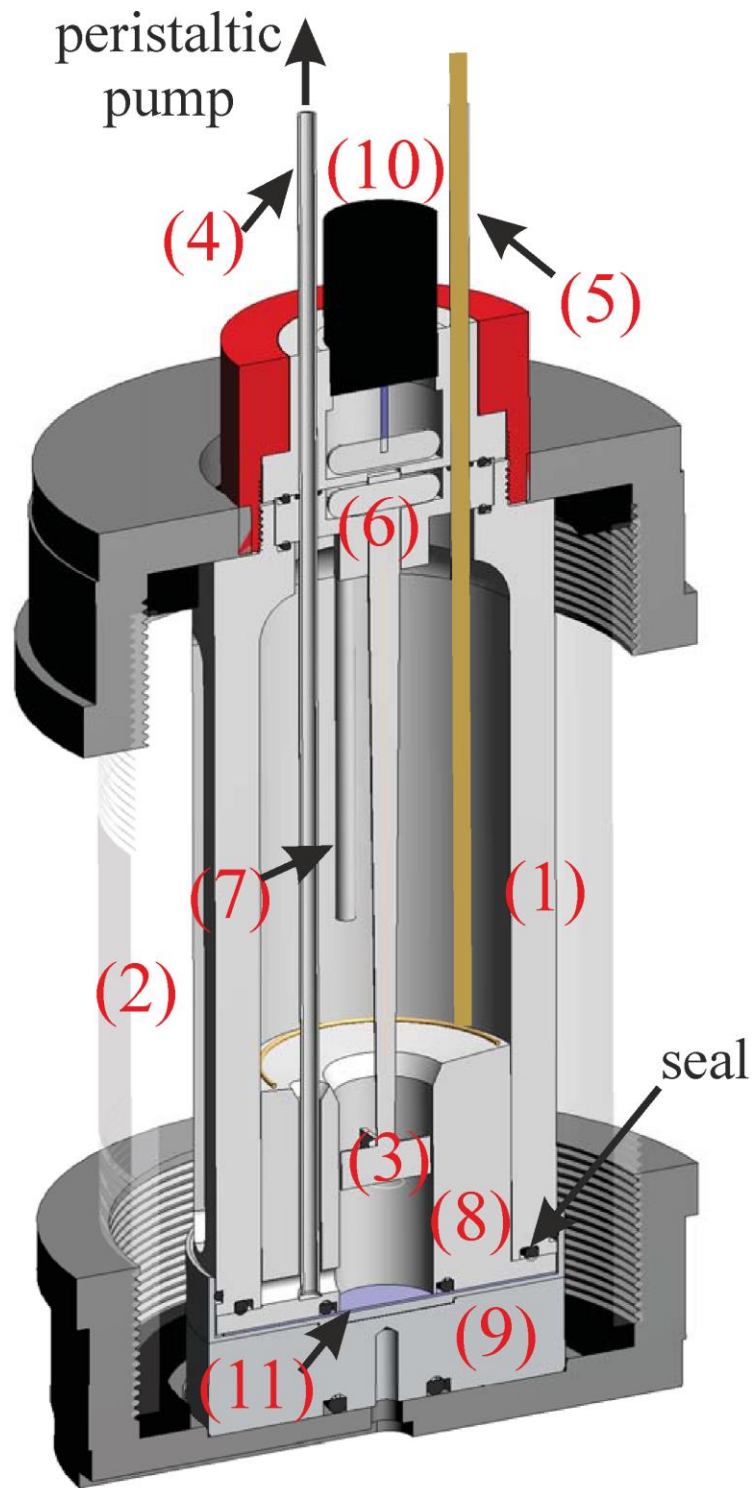


*Fig. 1 Anodization cell: (1) inner container (2) outer container (3) stirring bar (4) Pt-tube (5) Pt-cathode (6) magnetic coupling (7) exhaust (8) high-current adapter (9) Al-anode (10) motor (11) Si wafer*

Fig. 1 shows a cutaway drawing of the etching cell with the most important components of the cell. These are the inner and outer electrolyte containers, the aluminum and platinum electrodes, the stirring bar with its drive motor, a platinum tube and several hydrofluoric-acid-resistant seals.

The primary electrolyte container is the central part of the etching cell. This vessel is made from Teflon to avoid any contamination of the electrolyte due to chemical reactions with the wall material. Its inner dimensions are 55 mm in diameter and 135 mm in height. During cell operation, this vessel holds between 150 ml and 320 ml of the electrolyte for the synthesis of the porous silicon samples. Such a large volume of the primary container reduces the necessity of refilling and exchange of the electrolyte during the synthesis process and thus enables rather long etching times corresponding to increased sample thickness. The starting material for the synthesis of porous silicon, a bulk single-crystalline silicon wafer with a diameter of 76 mm, is mounted at the bottom of the vessel. Here, an aluminum bottom plate, which acts as an electrode provides a single electrical contact for anodization. The electrochemically formed porous epilayer does not reach the bottom of the silicon wafer. The remaining bulk silicon forms the blockade between the electrolyte and the electrode. Two HF-resistant seals reliably prevent HF-leakage from the electrolyte reservoir and consequently prevent any electrolyte-electrode contact. Note that this article is by no means a thorough and complete introduction into the safety requirements for HF-anodization. Here, we present a novel etching cell, which we think provides a higher degree of safety for experimentalists.

An access port, also made from Teflon, seals the top of the primary electrolyte container by another two seals. Three feedthroughs located at this exit port allow for electrical contact, electrolyte transfer and venting. A platinum ring electrode with adjustable height is located inside the container, respectively inside the electrolyte roughly 50 mm above the silicon wafer. This O-ring sealed ring electrode provides a feedthrough for electrical contact penetrating the access port. A platinum tube with an inner diameter of 3 mm extends into the inner vessel. The HF-resistant Pt tube, which is adjustable in height allows for filling and removing the electrolyte via the access port as well as for cleaning of the cell post-etching with water or other suitable solvents. The inner vessel also hosts a stirring bar made of Teflon. The stirring bar is magnetically coupled to the drive motor on top of the access port (Fig. 1). During operation, it permanently circulates the electrolyte and guarantees a spatially homogeneous electrolyte for well-defined etching conditions. The third and last feedthrough is used as exhaust for gaseous hydrogen produced during the synthesis.

A secondary containment encapsulates the inner vessel with the stirring bar, the Pt-electrode, the pumping tube, the silicon wafer and the aluminum electrode. Its main parts are a transparent PVC-U tube combined with two protecting caps. The tube is made of transparent PVC-U with temporary HF-resistivity and threaded at both ends to attach the caps. Its inner diameter is 114 mm with a wall thickness of 6.37 mm. During normal operation, the two HF-resistant seals introduced above separate primary and secondary electrolyte container. However, in the case of an inner leak, the secondary containment provides a buffer volume of 300 cm<sup>3</sup> to prevent a hazardous, dangerous HF spill into the environment.

The threaded tube and the protection caps facilitate a screw-less design of the etching cell. They allow for adjusting the appropriate pressure on the seals between the silicon wafer and the primary electrolyte container as well as on the seal between the primary container and the access port. The entire cell design minimizes electrolyte evaporation. In particular, selective evaporation of electrolyte components (HF, ethanol) that changes the electrolyte composition is significantly reduced leading to little variation of the process conditions. In turn, these stable long-time etching conditions allow for the synthesis of samples with huge thicknesses into the millimeter range. Such large samples, which retain macroscopic single-crystallinity [17, 39] despite the nanopore structuring, opening up the avenue towards a whole range of experiments hitherto not possible. For example, new insights of heat transport or elastic properties can be gained by the study of phonon properties by such as phonon dispersion

[44] or phonon lifetimes [45]. Due to the flux limitation of neutron sources these experiments are indeed demanding in terms of sample volume.

#### **Electrolyte Transfer:**

A peristaltic pump [46] connects the primary electrolyte container of the etching cell with various liquid reservoirs via elastic tubing (Fig. 2). Depending on the particular process step, these reservoirs are either the electrolyte reservoir, the waste disposal container or diverse solvent containers to transfer and remove liquids to and from the cell.

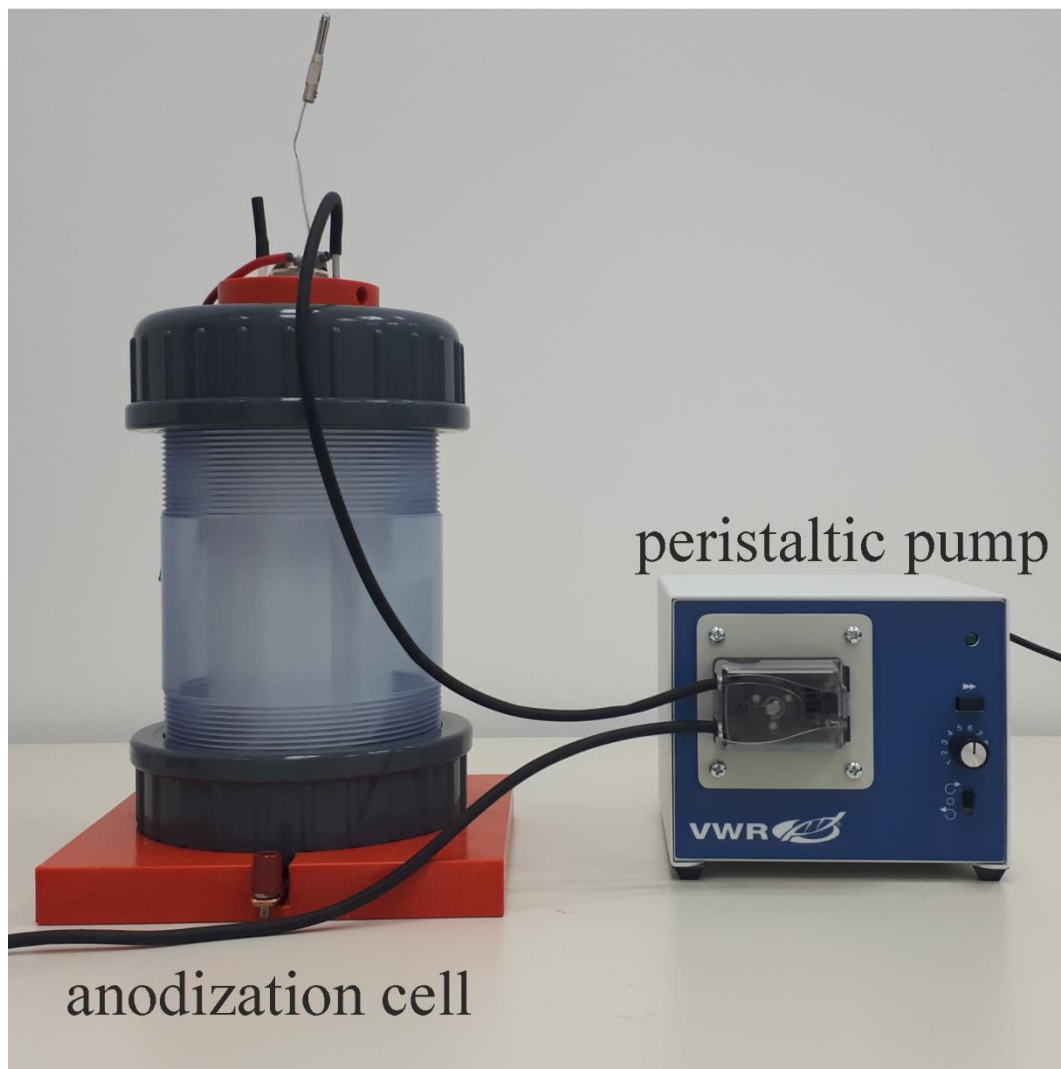


*Fig. 2 Anodization cell and peristaltic pump*

The present setup utilizes a fluoroelastomer tube with an inner diameter of 2.79 mm that is well suited for pumping hot and highly corrosive liquids [47]. In order to ensure that the sample morphology is not altered by excessive contact to the electrolyte it is important to remove the electrolyte promptly after the synthesis is completed, i.e. as soon as the electrical current is switched off. With the current pump model and tubing, it takes about 10 min to fill (or empty) the electrolyte vessel with 150 ml of electrolyte, which is adequate for the current

application. Peristaltic pumps with a larger flow rate are available, which would allow to reduce the time for filling and removal of the electrolyte liquids to less than one minute.

The concept of peristaltic pumping relies on the cyclic compression and relaxation of the flexible tubing. This is a mechanically demanding process, which quickly leads to material fatigue. Given the potential risk of a leakage in the tubing during electrolyte transfer or sample synthesis it is highly recommended to exchange the fluoroelastomer tubing in the apparatus in regular intervals. Good experience for reliable operation is made when exchanging the tubing after 10 hours of exposure to HF (48%) : Ethanol (99.99%) in 4:6 ratio electrolyte.

### Software Control:

A highly adaptable LabVIEW™-based software monitors and controls the anodization process. This software provides a direct interface to operate the power supply, Ampere meters and Voltmeters used for anodization. It records and time-stamps the current density and the applied voltage bias during etching. Customized anodization sequences with time-dependent current density or etching voltage can be readily defined within the input mask of the graphical user interface. Various etching conditions can result in different pore morphologies [1, 7, 37-39] that are desired for applications therefore this mode is a great advantage of our set-up.

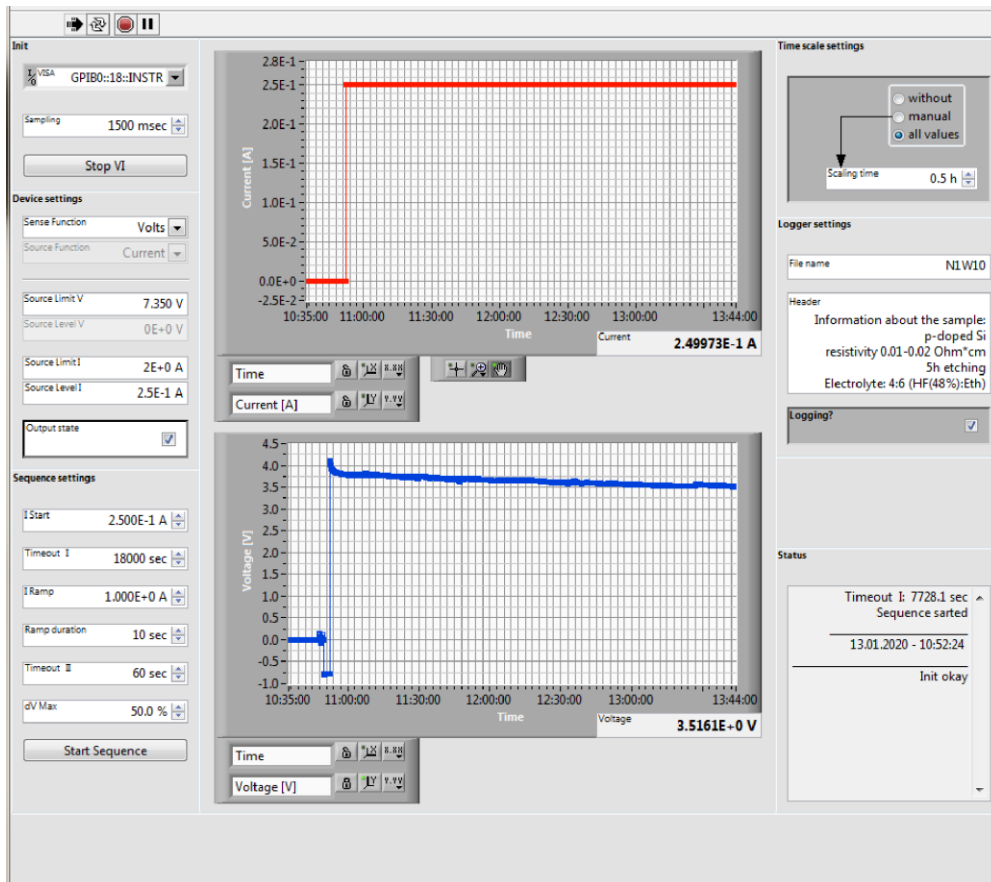


Fig. 3 Graphical user interface: The settings start an anodization sequence with constant-current of 250 mA for 18000 s. Subsequently, the current is increased to 1A within 10 s to detach a porous membrane form the source wafer. The detaching current is turned off after 60 s.

The graphical user interface of the control software is shown in Fig. 3. The two graphs in the panel display the time dependence of the anodization current, which is kept constant during synthesis and the voltage, which slowly decreases with time as a result of varying concentration of mobile ions in the electrolyte. The input mask shows user defined parameters for a constant-current etching profile to synthesize a mesoporous Si membrane. In order to produce a free-standing membrane, the current needs to be raised for a short time right at the end of the synthesis process. The thus enlarged pore size leads to enhanced interconnection of the pores finally leading to the separation of the mesoporous membrane from the remaining bulk Si wafer.

### **Electrochemical Synthesis of Porous Silicon, Cell Operation:**

Electrochemical anodization of single-crystalline silicon wafers is a versatile approach to synthesize micro- and mesoporous silicon [7]. The control parameters for the etching process fall into three categories: properties of the source material, the electrolyte composition and the anodization conditions. Single-crystalline silicon wafers with p-type or n-type doping, different doping levels and different crystallographic orientations lead to different pore morphologies [37]. Likewise, different electrolyte compositions, concentrations and temperatures cause different porosities, pore size distributions, specific surface areas and overall different pore networks. An efficient and widely used electrolyte for etching under constant current density conditions is hydrofluoric acid mixed with different solvents, like ethanol or methanol. Tuning the etching time and current density has a similar impact on the anodization result. We refer the interested reader to references [1, 7, 38, 39], which give a comprehensive discussion of the influence of the various control parameters on the obtainable sample morphology. The electrochemical oxidation and reduction processes at the electrolyte silicon interface that trigger the pore growth during anodization are described comprehensively in references [39-42].

In detail, the synthesis sequence for micro- and mesoporous silicon utilizing the novel cell consists of the following steps: 1. Assembling of the cell, 2. connecting the electrodes to the current source, 3. defining the etching parameters in the control software, 4. electrolyte pumping from the reservoir to the primary containment, 5. starting the etching process by the control software, 6. pumping the electrolyte from the etching cell to a waste disposal container, 7. flushing the primary vessel multiple times with water and solvents via peristaltic pumping, 8. disassembling the cell to remove the sample, and 9. sample cleaning.

To illustrate the performance of the novel etching cell we have characterized a mesoporous Si sample synthesized with the apparatus described. As starting material we used a 375  $\mu\text{m}$  thick, p-doped Si wafer purchased from Si-Mat and specified to have a resistivity  $\rho = 0.01\text{-}0.02 \Omega \text{ cm}^{-1}$ . The wafer was oriented with the crystallographic [100] direction along the surface normal. Using an electrolyte mixture of 40 vol% hydrofluoric acid (48% concentration) and 60 vol% ethanol (99.99%) this wafer has been anodized for 5 hours with a constant current density of 13  $\text{mA/cm}^2$ . The synthesis process resulted in a 200  $\mu\text{m}$  thick porous epi-layer on bulk silicon as has been confirmed by optical microscopy (see Fig. 4, top left). SEM micrographs demonstrate the mesoporous morphology of the sample (Fig. 4 top right). For a volume-sensitive, quantitative characterization of the average pore diameter, the pore size distribution and the porosity we used  $\text{N}_2$  sorption isotherm measurements [43]. These measurements confirm a rather narrow pore size distribution with an average pore diameter of 8 nm. A porosity of 60% is obtained for the present sample.

The apparatus allows also to perform a long etching synthesis. To demonstrate this possibility we prepared a porous epilayer with the thickness in a millimeter range (Fig. 5). The thickness of the layer is reduced by about 10% over the last few millimeters towards the edge. Similar than the thickness of the epilayer, its porosity changes only close to the edge. At the boundary of the epilayer the relative change in porosity amounts to approximately 20%.

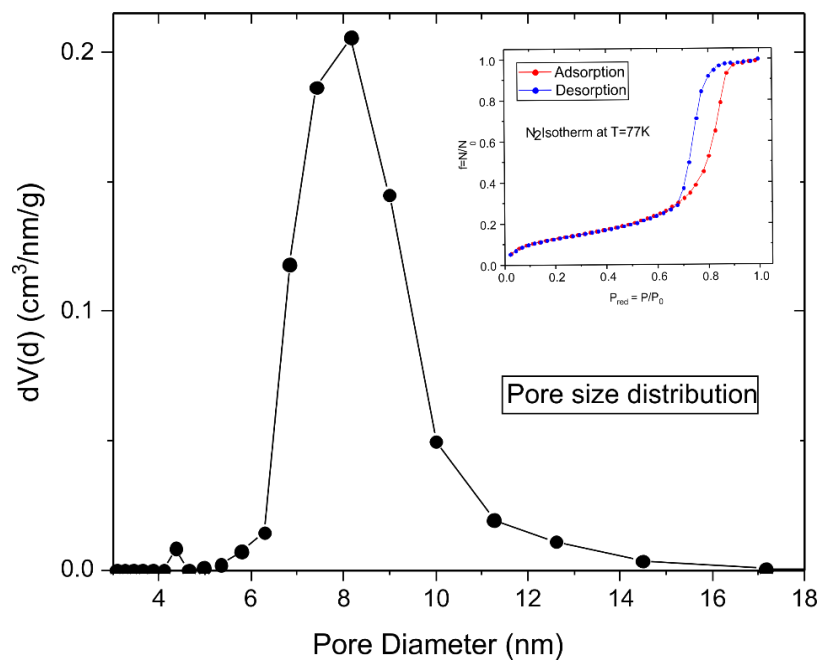
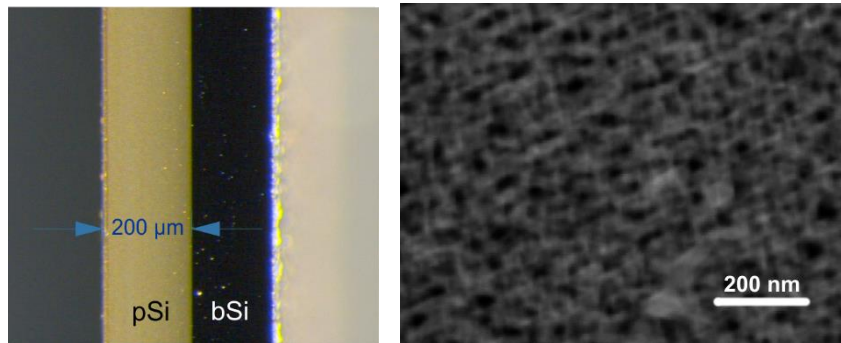
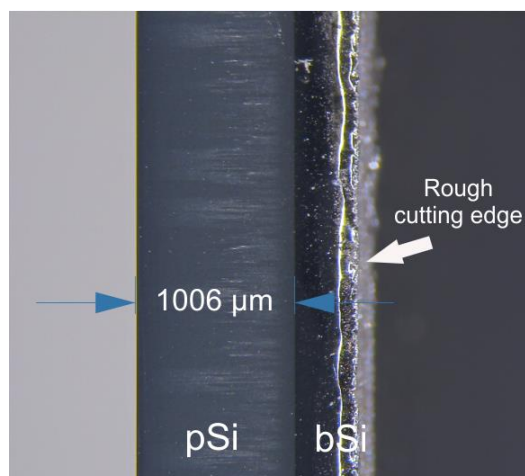


Fig. 4 Optical microscopy image of a porous epi-layer (top left), SEM micrograph of epi-layer (top right), pore-size distribution (bottom) and N<sub>2</sub> sorption isotherm (inset)



*Fig. 5 Optical microscopy image of a 1006  $\mu\text{m}$  thick porous epi-layer. The sample was etched in a 8:2 HF(48%):Eth solution with a constant current density of 13  $\text{mA}/\text{cm}^2$  for 29 hours.*

**Summary:**

This article presented a novel anodization cell for the synthesis of micro- and mesoporous silicon by electrochemical etching using hydrofluoric-acid-based electrolytes. The cell's primary and secondary safety containment for the electrolyte in combination with a closed peristaltic pumping system for the electrolyte transfer guarantee an improved and safe working environment for experimentalists performing Si anodization. The presented control software allows for more complicated, time-dependent etching sequences and provides a high degree of flexibility for the operator to control and adapt the etching process. The entire cell design was optimized to perform both, short-time etching up to several minutes as well as long-time etching over several days. An obvious upgrade path for the cell is the implementation of a continuous flow mode. So far, long-time etching relies on an appropriate amount of electrolyte in the primary container. Under continuous flow, the electrolyte in the cell is then permanently replenished by means of peristaltic pumping and an external electrolyte reservoir to achieve a time-independent electrolyte concentration during long-time etching processes.

**Data availability statement:**

All data relevant for this study can be found in the article. The corresponding author can be contacted anytime when a reader needs additional information.

**Acknowledgement:**

We thank the DFG for funding the project 'Hybrid thermoelectrics based on porous silicon: Linking Macroscopic Transport Phenomena to Microscopic Structure and Elementary Excitations', project number 402553194.

REFERENCES

- [1] V. Lehmann, R. Stengl, and A. Luigart, *Mater. Sci. Eng. B*, 69, 11 (2000).
- [2] L. D. Chen *et al.*, *J. Appl. Phys.*, 90, no. 4, 1864 (2001).
- [3] S. LeBlanc, *Sustain. Mater. Technol.*, 1, 26 (2014).
- [4] A. Janshoff, K.S. Dancil, C. Steinem, D. P. Greiner, V. S.-Y. Lin, C. Gurtner, K. Motesharei, M. J. Sailor, M. R. Ghadiri, *J. Am. Chem. Soc.*, 120, 12108 (1998).

- [5] P. Huber, *J. Phys. Condens. Matter*, 27, 103102 (2015).
- [6] M. Ashuri, Q. He, and L. L. Shaw, *Nanoscale*, 8, 74 (2016).
- [7] M. J. Sailor, *Porous Silicon in Practice: Preparation, Characterization and Applications*, Wiley, 2012.
- [8] L. Velleman, J. Shearer, V. Ellis, D. Losic, H. Voelcker, and J. George, *Nanoscale*, 2, 1756 (2010).
- [9] E. Alleno, L. Chen, C. Chubilleau, B. Lenoir, O. Rouleau, M. F. Trichet and B. Villeroy, *J. Electron. Mater.*, 39, 1966 (2010).
- [10] S. H. C. Anderson, H. Elliott, D. J. Wallis, L. T. Canham, and J. J. Powell, *Phys. Status Solidi*, 197, 331 (2003).
- [11] J. De Jong, R. G. H. Lammertink, and M. Wessling, *Lab Chip*, 6, 1125 (2006).
- [12] H. Kim, B. Han, J. Choo, and J. Cho, *Angew. Chem. Int. Ed.*, 47, 10151 (2008).
- [13] M. Ge, J. Rong, X. Fang, and C. Zhou, *Nano Lett.*, 12, 2318 (2012).
- [14] P. Menna, G. Di Francia and V. La Ferrara, *Solar Energy Materials and Solar Cells* 37, 13 (1995).
- [15] J. H. Petermann, D. Zielke, J. Schmidt, F. Haase, E. G. Rojas and R. Brendel, *Prog. Photovolt: Res. Appl.*, 20, 1 (2011).
- [16] H. So and A. P. Pisano, *Int. J. Heat Mass Transf.*, 89, 1164 (2015).
- [17] J. de Boor, D. S. Kim, X. Ao, M. Becker, N. F. Hinsche, I. Mertig, P. Zahn and V. Schmidt, *Appl. Phys. A Mater. Sci. Process.*, 107, 789 (2012).
- [18] J. Tang, H. Wang, D. Hyun Lee, M. Fardy, Z. Huo, T. P. Russell, P. Yang, *Nano Lett.*, 10, 4279 (2010).
- [19] G. Schierning, *Phys. Status Solidi A*, 211, 1235 (2014).
- [20] C. Hong, J. Lee, H. Zheng, S. Hong, and C. Lee, *Nanoscale Res. Lett.*, 6, (2011).
- [21] A. Ressine, I. Corin, K. Järås, G. Guanti, C. Simone, G. Marko-Varga, T. L. Professor, *Electrophoresis*, 28 4407 (2007).
- [22] R. Guégan, D. Morineau, R. Lefort, A. Moréac, and W. Béziel, *J. Chem. Phys.*, 126, 064902 (2007).
- [23] R. Busselez, R. Lefort, M. Guendouz, B. Frick, O. Merdrignac-Conanec, and D. Morineau, *J. Chem. Phys.*, 130, (2009).
- [24] R. Guégan, D. Morineau, R. Lefort, W. Béziel, M. Guendouz, L. Noirez, A. Henschel and P. Huber, *Eur. Phys. J. E*, 26, 261 (2008).
- [25] L. Canham, *Handbook of Porous Silicon*. 2014.
- [26] S. Borini, A. M. Rossi, L. Boarino, and G. Amato, *J. Electrochem. Soc.*, 150, G311 (2003).
- [27] A. Küller, W. Eck, V. Stadler, W. Geyer, and A. Götzhäuser, *Appl. Phys. Lett.*, 82, 3776 (2003).
- [28] W. Chen and A. Haroon, *Appl. Phys. A Mater. Sci. Process.*, 62, 1499 (1993).
- [29] C. Chang, Y.-F. Wang, Y. Kanamori, J.-J. Shih, Y. Kawai, C.-K. Lee, K.-C. Wu and M. Esashi, *J. Micromechanics Microengineering*, vol. 15, 2005.
- [30] Y. Hirai, H. Yabu, Y. Matsuo, and M. Shimomura, *J. Mater. Chem.*, 20, 10804 (2010).
- [31] C. Chartier, S. Bastide, and C. Lévy-Clément, *Electrochim. Acta*, 53, 5509 (2008).

- [32] X. Li and P. W. Bohn, *Appl. Phys. Lett.*, 77, 2572 (2000).
- [33] Z. Huang, N. Geyer, P. Werner, J. de Boor, and U. Gösele, *Adv. Mater.*, 23, 285 (2011).
- [34] A. V. Kabashin and M. Meunier, *Appl. Surf. Sci.*, 186, 578 (2002).
- [35] Z. Zhang, Y. Wang, W. Ren, Q. Tan, Y. Chen, H. Li, Z. Zhong and F. Su *Angew. Chem.*, 126, 5265 (2014).
- [36] R. E. Hummel and S.-S. Chang, *Appl. Phys. Lett.*, 61, 1965 (1992).
- [37] R. Herino, G. Bomchil, K. Barla, and C. Bertrand, *J. Electrochem. Soc.*, 134, 1994 (1987).
- [38] E. V. Astrova, T. N. Borovinskaya, A. V. Tkachenko, S. Balakrishnan, T. S. Perova, A. Rafferty and Y. K. Gun'ko, *J. Micromechanics Microengineering*, 14 1028 (2004).
- [39] X. G. Zhang, *J. Electrochem. Soc.*, 151, 2004.
- [40] R. L. Smith and S. D. Collins, *J. Appl. Phys.*, 71, R1 (1992).
- [41] P. C. Searson, J. M. Macaulay, and S. M. Prokes, *J. Electrochem. Soc.*, 139, 3373 (1992).
- [42] P. C. Searson, J. M. Macaulay, and F. M. Ross, *J. Appl. Phys.*, 72, 253 (1992).
- [43] E. P. Barrett, L. G. Joyner, and P. P. Halenda, *Vol. Area Distributions Porous Subst.*, vol. 73, 373 (1951).
- [44] T. Hofmann, D. Wallacher, R. Toft-Petersen, B. Willenberg, M. Reehuis, and K. Habicht, *Microporous and Mesoporous Materials*, 243, 263 (2017).
- [45] K. Habicht, Habilitation thesis „Neutron-Resonance Spin-Echo Spectroscopy: A High Resolution Look at Dispersive Excitations“, Universität Potsdam 2017.
- [46] <https://sg.vwr.com/store/product/17880316/peristaltic-pumps-pp-10-and-pp-20>
- [47] <https://sg.vwr.com/store/product/577652/tubing-for-auto-analyser-fluran-f-5500-a>
- [48] C. R. Ocier, N. A. Krueger, W. Zhou, and P. V. Braun, Tunable Visibly Transparent Optics Derived from Porous Silicon, *ACS Photonics*, 4, 909 (2017)
- [49] V. Robbiano, G. M. Paternò, A. A. La Mattina, S. G. Motti, G. Lanzani, F. Scotognella and G. Barillaro, *Room-Temperature Low-Threshold Lasing from Monolithically Integrated Nanostructured Porous Silicon Hybrid Microcavities*, *ACS Nano*, 12, 4536 (2018)
- [50] S. Mariani, V. Robbiano, L. M. Strambini, A. Debrassi, G. Egri, L. Dähne and G. Barillaro., *Layer-by-layer biofunctionalization of nanostructured porous silicon for high-sensitivity and high-selectivity label-free affinity biosensing*, *Nat. Commun.*, 9 , 5256 (2018)